

Inelastic analysis of reinforced concrete panels: experimental verification and application

Autor(en): **Cervenka, Vladimir / Gerstle, Kurt H.**

Objektyp: **Article**

Zeitschrift: **IABSE publications = Mémoires AIPC = IVBH Abhandlungen**

Band (Jahr): **32 (1972)**

PDF erstellt am: **13.09.2024**

Persistenter Link: <https://doi.org/10.5169/seals-24951>

Nutzungsbedingungen

Die ETH-Bibliothek ist Anbieterin der digitalisierten Zeitschriften. Sie besitzt keine Urheberrechte an den Inhalten der Zeitschriften. Die Rechte liegen in der Regel bei den Herausgebern.

Die auf der Plattform e-periodica veröffentlichten Dokumente stehen für nicht-kommerzielle Zwecke in Lehre und Forschung sowie für die private Nutzung frei zur Verfügung. Einzelne Dateien oder Ausdrucke aus diesem Angebot können zusammen mit diesen Nutzungsbedingungen und den korrekten Herkunftsbezeichnungen weitergegeben werden.

Das Veröffentlichen von Bildern in Print- und Online-Publikationen ist nur mit vorheriger Genehmigung der Rechteinhaber erlaubt. Die systematische Speicherung von Teilen des elektronischen Angebots auf anderen Servern bedarf ebenfalls des schriftlichen Einverständnisses der Rechteinhaber.

Haftungsausschluss

Alle Angaben erfolgen ohne Gewähr für Vollständigkeit oder Richtigkeit. Es wird keine Haftung übernommen für Schäden durch die Verwendung von Informationen aus diesem Online-Angebot oder durch das Fehlen von Informationen. Dies gilt auch für Inhalte Dritter, die über dieses Angebot zugänglich sind.

Inelastic Analysis of Reinforced Concrete Panels: Experimental Verification and Application¹⁾

*Analyse non-élastique de plaques acier-béton:
Vérification expérimentale et application*

*Unelastische Analyse von Stahlbetonscheiben:
Experimentelle Nachprüfung und Anwendung*

VLADIMIR CERVENKA

Structural Engineer, Building Research
Institute, T. U. Prague, formerly, Re-
search Assistant, University of Colorado,
Boulder

KURT H. GERSTLE

Professor of Civil Engineering, University
of Colorado, Boulder

Introduction

The analysis described in a previous paper [1] provides an approximate solution for the inelastic response of reinforced concrete panels. This analysis is based on the incremental finite element method and includes two types of material nonlinearities, namely, crack propagation and plasticity.

Two kinds of unavoidable approximations were introduced in this analysis, namely, material behavior idealization and discrete numerical solution. The effect of these approximations is studied here by means of analytical and experimental results.

Two test series were used for this purpose in this investigation. The first test series, intended to simulate the action of shear walls, was conducted by the authors, the second test series was performed by T. PAULAY [2] in connection with an investigation of the coupling of shear walls. The full description of the comparative study is given in Ref. [3]. Here, only representative results are shown to illustrate the conclusions.

¹⁾ This material is presented in two parts. The first paper published in Vol. 31-II describes the theoretical aspects. This is the second paper which presents experimental verification and application to shear walls.

The specimens used in both studies were deep beams subjected to the maximum moment M and shear force V . Such a loading can be characterized by the shear span ratio r defined by $r = \frac{M}{Vd}$, where d is the depth of the beam. The shear span ratio in the first test series was approximately $r = 1$, and the shear span ratio in Paulay's coupling beams was $r = 0.5$. Both of these ratios indicate relatively large shear loading.

In practical structural design, wall elements such as shear walls or deep beams are often treated by methods developed for ordinary beams. Results of these beam solutions will be compared with the finite element analysis and experiments, in order to judge their validity.

Authors' Tests

The purpose of the experimental program was to provide data on the real behavior of reinforced concrete panels under in-plane loads which could be compared with the analytical results. The following aspects were mainly investigated:

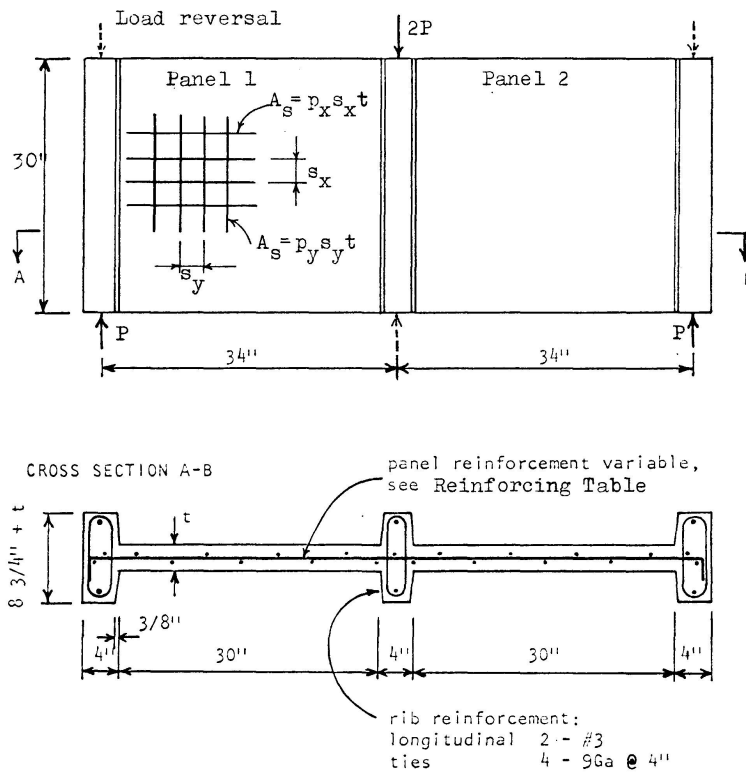
1. The load-displacement response of panels.
2. The crack patterns and crack propagation.
3. Failure mechanisms.

The test panels were orthogonally reinforced square plates 30×30 in., 2 or 3 inches in thickness, reinforced as indicated in Fig. 1. Two panels were combined to form one beam-like specimen as shown in Fig. 1; this arrangement enabled testing of the beam specimen as a simply supported beam with mid-point load. Thus, two square panels were always tested simultaneously, though each panel acted independently of the other because of the statically determinate supports. The concentrated forces at the supports and at the load point were transmitted to the panels by three vertical ribs as shown in Fig. 1. These ribs also helped to maintain the lateral stability of the specimens during the testing.

The testing arrangement allowed application of monotonic as well as cyclic load histories.

Horizontal and vertical displacements were measured at the bottom point of the outside ribs. Direct relative displacements of the panel corners with respect to the top of the center rib were obtained.

The cracks were continuously observed, and new cracks were marked. Pictures of the entire crack propagation were taken by two cameras, one for each panel. For easier identification of the crack location from the pictures, a mesh coinciding with the finite element mesh considered in the analysis was drawn on the surface of the panel.

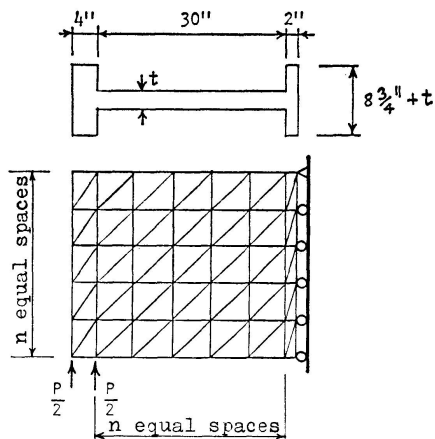


Panel	Thick-ness t , in.	Reinforcing					
		Type	s_x , in.	p_x	s_y , in.	p_y	
W 2	3	# 3	4	0.00916	4	0.00916	Top. 24" Bot. 6"
			2	0.01832			
W 3-2	2	1/4" Rod	2	0.00785	-	-	
W 4	3	# 3	3	0.0122	3	0.0122	

Fig. 1. Test Specimen.

Analytical Models

The test specimens were analyzed by the finite element method described in a previous paper [1]. The idealization of the panel shown in Fig. 1, for the finite element analysis is shown in Fig. 2. Three types of finite element meshes, M_n , with $n = 5, 8,$ and 10 were used. All supports are located along the right vertical boundary line where all but the topmost nodal point are constrained horizontally and free vertically; the topmost nodal point is constrained in both directions. The actual single load P , acting on each panel, is substituted by two equivalent loads $P/2$.



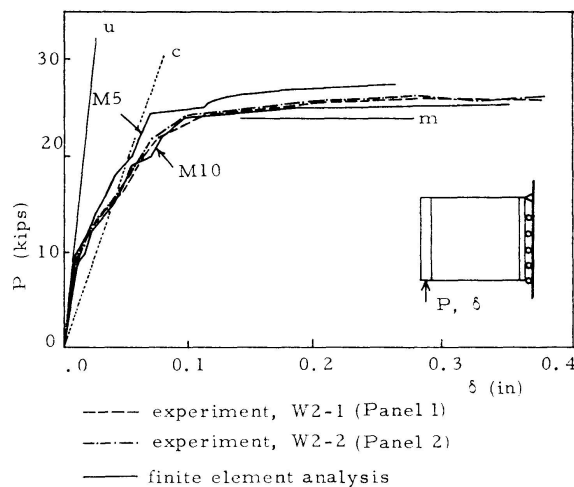
n	Designation	Number of Elements
5	M 5	70
8	M 8	160
10	M 10	240

Fig. 2. Finite Element Model.

Analytical and Experimental Results

Specimen W 2

Experimental load-displacement diagrams for both panels of specimen *W 2* are shown in Fig. 3. The load P on the panel is plotted versus the vertical displacement of the outside rib at the point of load P .

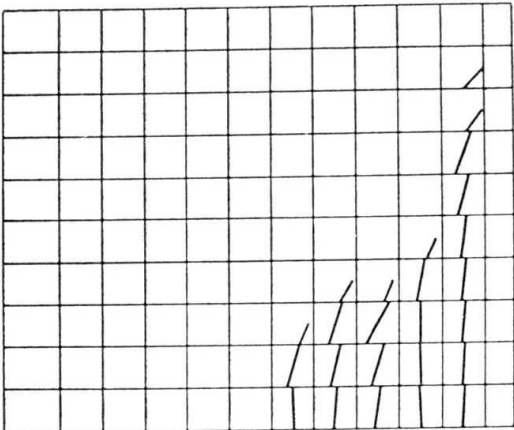
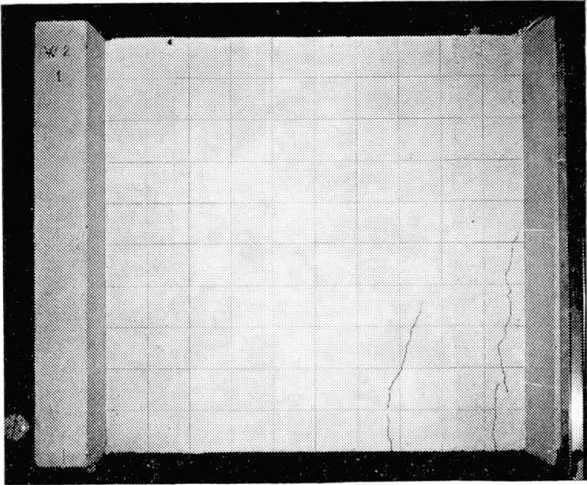
Fig. 3. Comparison of Analytical and Experimental Load-Displacement Diagrams for Specimen *W 2*.

The finite element analysis of this specimen was performed for two kinds of meshes, *M 5* and *M 10*, to show the effect of the size of finite element. The load-displacement diagrams for both meshes are also shown in Fig. 3. As expected from the bound principles of the displacement method, the finer grid results in increased deformations. Both analyses were terminated by specifying limit displacements. At these points the load-displacement diagrams were almost horizontal and no further increase of load was expected.

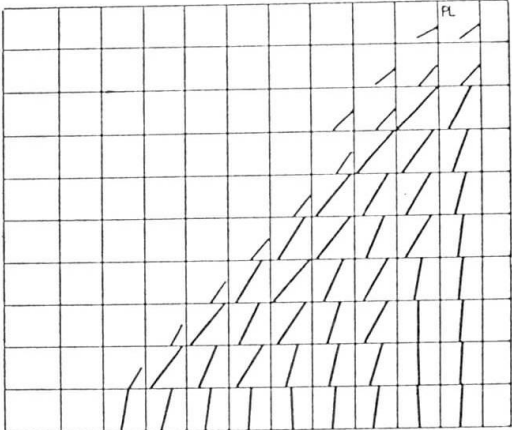
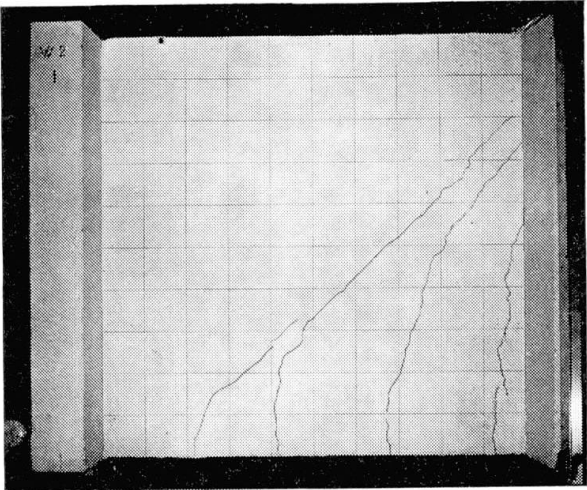
Fig. 3 also shows lines representing predictions based on beam theory.

Experiment

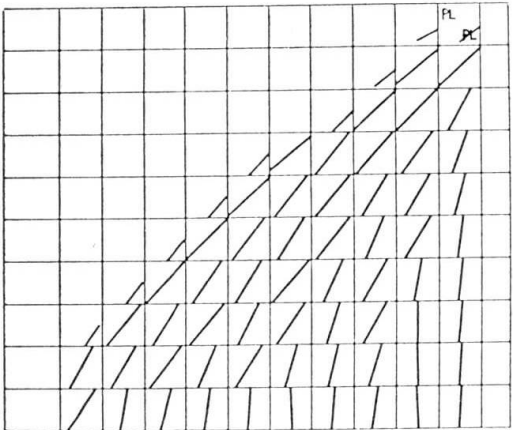
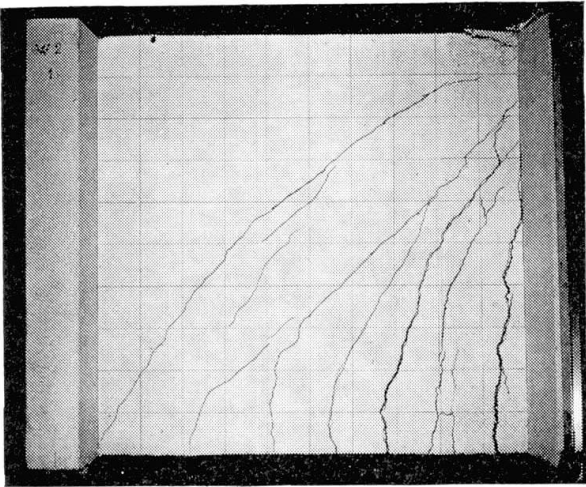
Analysis



a) $P = 14.0$ Kips



b) $P = 24.0$ Kips



c) $P = 25.5$ Kips

Fig. 4. Comparison of Analytical and Experimental Crack Patterns for Panel W 2.

Lines u and c represent elastic beam behavior based, respectively, on uncracked and cracked section properties. Line m represents ultimate load due to attainment of the ultimate bending moment at the critical section. It can be observed here that beam theory yields reasonably good results.

Analytical and experimental crack patterns for three load levels are shown in Figs. 4a to c. The agreement between analytical $M 10$ and experimental results is excellent for load-displacement relationship as well as for crack locations and crack directions.

From the test it was observed that the flattening of the load-displacement diagram was initiated by yielding of the reinforcement which was indirectly evident from the wide opening of the cracks at $P = 24 K$ and $\delta = 0.1$ inch. The failure of the test specimen was caused by crushing of the concrete at $P = 27 K$ and $\delta = 0.45$ inch. This type of failure was very well predicted by the analysis. The maximum concrete compression strain in the plastic zone (designated by PL in Fig. 4c) at the last calculated load stage $P = 25.5 K$ and $\delta = 0.35$ in. was $\epsilon^c = 0.0087$. If the limit concrete strain is assumed $\epsilon_u \leq 0.008$ the analysis would predict crushing of the concrete and consequent failure of the panel at that stage. The failure of the test panel was observed under slightly higher load and greater displacement at $P = 26.5 K$ and $\delta = 0.45$, which is considered to be in a good agreement with analytical values.

Specimen W 3

This specimen contained panels with different reinforcement. Panel $W 3-1$ was reinforced orthogonally and panel $W 3-2$ had only horizontal reinforcement. Failure of the specimen was caused by the weaker panel $W 3-2$. Only results for this panel will be presented here.

Three different analyses were performed and compared with the experimental behavior.

In the first analysis the force increments were specified. The load-displacement diagrams of this analysis and experiment are compared in Fig. 5 and the final crack patterns are compared in Fig. 6. Good agreement between analytical and experimental behavior is found over the entire load range except in the limit stage.

The failure mechanism observed from the experiment was of a typical shear type, characterized by opening of one diagonal crack, as shown in Fig. 6. It can be seen from the relative displacements of the mesh lines crossing the cracks that the diagonal crack opened in the vertical direction. This phenomenon can be also observed from the analysis as shown in Fig. 7. In this figure the analytical distribution of the strains ϵ_y along the vertical lines of the panel is shown; the points of maximum ϵ_y are connected to show the course of the predicted major diagonal crack, whose location agrees well with the observed crack. However, there is considerable difference between the mechanisms of

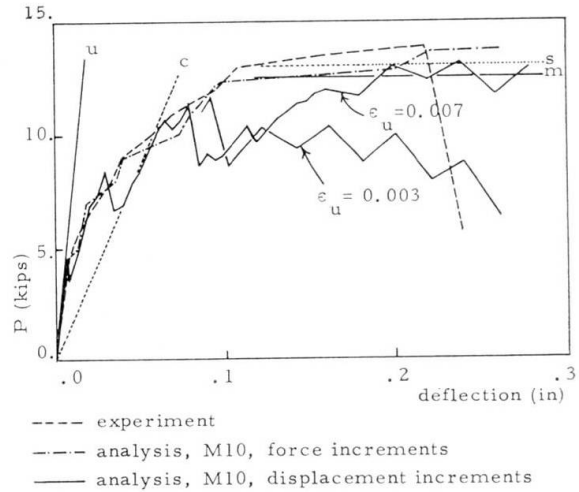
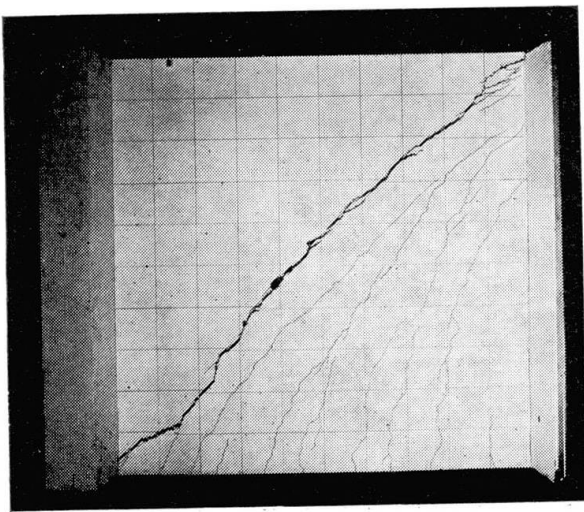
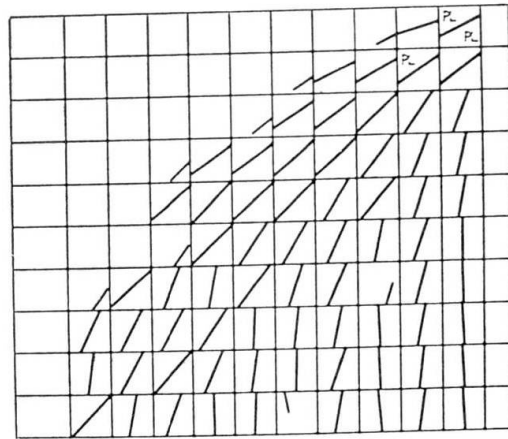


Fig. 5. Comparison of Analysis with Experiment for Panel W 3-2.



Experiment



Analysis

Fig. 6. Comparison of Final Analytical and Experimental Crack Patterns for Panel W 3-2.

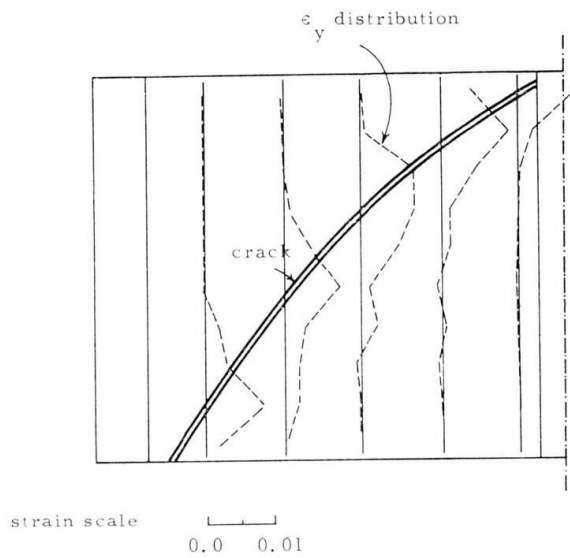


Fig. 7. Panel W 3-2. Diagonal Crack Location from the Distribution of Analytical Strains ϵ_y .

failure. While in the experiment the opening of the diagonal crack leads to an abrupt instability failure, the analysis shows plasticity of the cracked concrete in the vicinity of the diagonal crack which gives some additional displacement capacity to the panel.

The difference between the experimental and analytical failure mechanisms is caused mainly by the deficiency of the finite element representation of the cracked concrete. The analytical mechanism naturally results from the fact that the cracks are not smoothly continuous from one element to another, but form a sawtooth pattern; thus a continuous diagonal crack can form only if the concrete adjacent and parallel to the crack discontinuity is crushed.

Further analyses of the panel were performed for specified displacement increments. This type of analysis permits all instability regions characterized by drops of the load to be obtained. The resulting load-displacement diagrams for two values of compressive limit strain, $\epsilon_u = 0.003$ in/in and $\epsilon_u = 0.007$ in/in, are also shown in Fig. 5.

In these analyses the formation of diagonal cracks is accompanied by a big drop at $\delta = 0.08$ and 0.10 inches, respectively. A similar load drop due to diagonal crack opening in the experiment caused the failure at $\delta = 0.22$. It is seen that the analysis is indeed able to represent the loss of strength of the elements adjacent to the diagonal crack, if a sufficiently low ultimate concrete strain is assumed.

Fig. 5 also shows the lines u and c corresponding to the stiffnesses according to elastic, uncracked and cracked, beam theory with shear distortions included. The horizontal lines m and s indicate the ultimate beam strength in moment and shear, respectively. In this case also, beam theory can give reasonable results.

Specimen W 4

This specimen was subjected to cyclic loading. The comparison of analytical and experimental results is presented for the first four load cycles. One cycle includes loading and unloading in one direction. The load cycle in the positive direction was always followed by a load cycle in the reversed direction.

The magnitude of the cyclic load was $P = 12.0 K$ which is 0.46 of the monotonic limit load. The analysis of this cyclic loading is based on Mesch *M 8*. The comparison of analytical and experimental load-displacement diagrams for elastic cycling is shown in Fig. 8.

The analytical diagram indicates changes due to crack formation only in the first two cycles. In all following cycles with the same magnitude of load no other changes take place and the diagram is formed by the line connecting the origin and maximum load points. Hence, the analysis indicates elastic behavior of the cracked panel in the cycles following the first and second cycles. The experimental diagram shows some residual displacements even

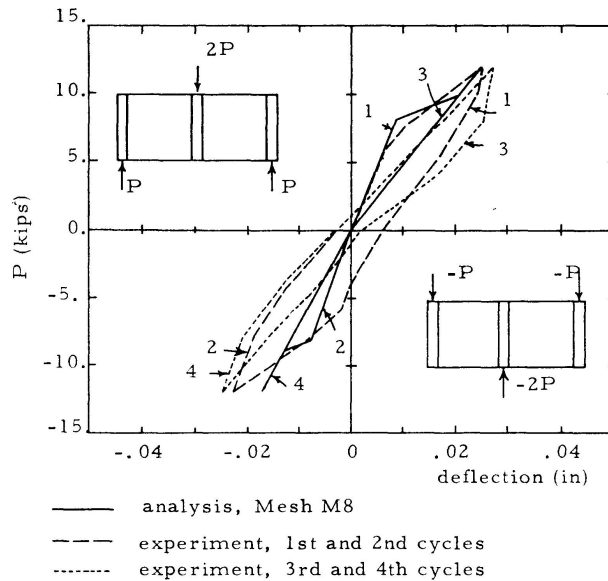


Fig. 8. Comparison of Analysis with Experiment for Specimen W 4 under Elastic Cycling. Numbers Indicate Cycles.

under this low load. These residual displacements are probably caused by bond slip and by imperfect crack closing caused by crack surface damage. All these effects are neglected in the analysis.

After completion of these four cycles the magnitude of load was increased and the specimen was subjected to cyclic loading of magnitude close to the limit monotonic load. Very large plastic deformations occurred during this loading and failure occurred in the sixth cycle. Clearly, a realistic analysis for cyclic loads in plastic range must include representation of bond slip and the crack mode with two sets of cracks opened simultaneously.

The crack patterns in both ranges of cyclic loading, which are not presented here, showed very good comparison between analysis and experiment.

Paulay's Tests

Two coupling beams were selected from (2) and used in the investigation. Here only one of them, Beam 391, is presented.

Test specimens were of the form shown in Fig. 9. The tested beam was connected with end blocks which simulated the real boundary conditions likely to occur in shear wall structures.

For purpose of the analysis the shape of the specimen was idealized as shown in Fig. 10. The stiffness of the end blocks was chosen such as to match the experimental stiffness in the elastic *uncracked* state. The analytical end rotations of beams are considered as rotations of the vertical line connecting the points 1 and 2 of Fig. 10. The experimental rotations were measured in the middle of the end blocks of the specimen shown in Fig. 9.

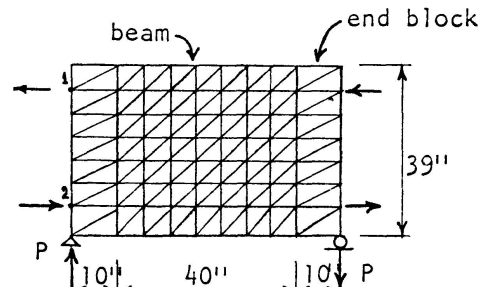
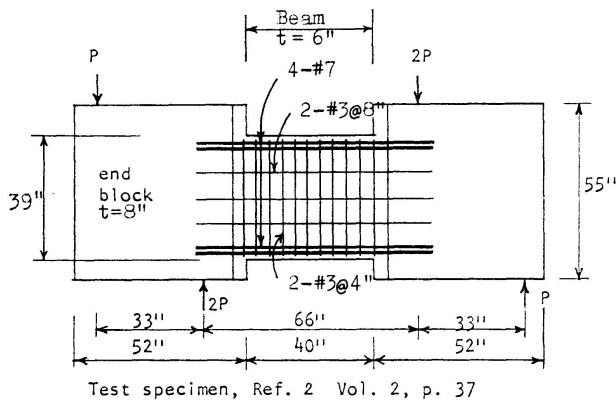


Fig. 10. Analytical Beam and Mesh Layout.

Fig. 9.

Beam 391

This beam was subjected to monotonically increasing load leading to failure. Two analytical solutions were performed, differing only in the tensile strength of concrete. The load-rotation diagrams of both solutions are compared with experimental results in order to show the effect of tensile strength on the solution. Two analytical curves, one using the modulus of rupture as a measure of the tensile strength, and the other using the splitting strength, are compared with experiment in Fig. 11. The analytical solutions differ only under low load when crack propagation takes place.

The analytical and experimental load-rotation diagrams indicate the overestimation of the real stiffness and of the real limit load by the analysis. This is partly caused by the coarseness of the finite element mesh. However, the main cause is probably the large bond slip of the main bending reinforcement

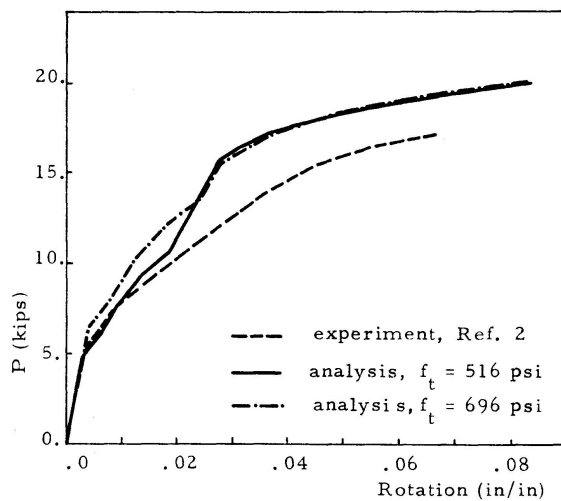
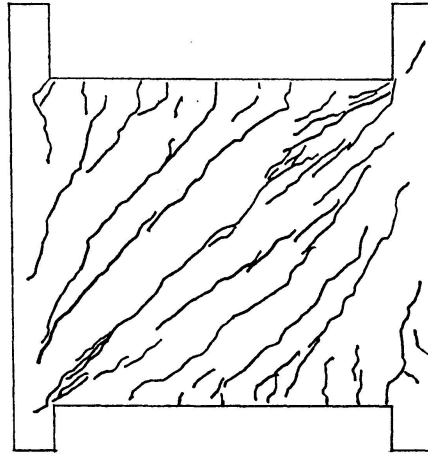


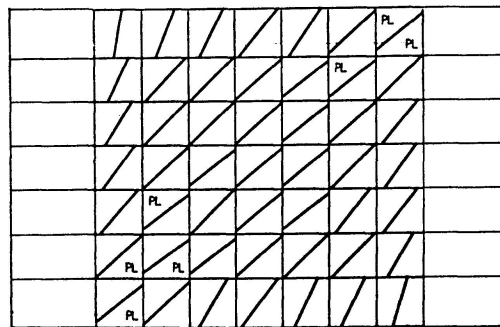
Fig. 11. Comparison of Analysis with Experiment for Beam 391.

(# 7 bars), particularly in the anchorage regions, which is not included in the analysis. Again it appears that inclusion of this effect in the analysis is necessary.

The comparison of the final analytical and experimental crack patterns is shown in Fig. 12.



Experimental Crack Pattern from Ref. 2, Vol. 2, p. 128.



Analysis

Fig. 12. Comparison of Analytical and Experimental Crack Patterns at Failure for Beam 391.

The experimental beam failed in shear when a major crack formed along the diagonal of the beam. Similarly to the case of Panel *W 3-2*, a discrepancy was found between analytical and experimental failure mechanisms. The continuous diagonal crack cannot form in the analytical solution due to the basic assumption of the method which considers every element separately. Instead, the analysis shows concrete plasticity in the vicinity of the beam diagonal, as indicated in Fig. 12.

The analytical and experimental strains in the top longitudinal steel are compared in Fig. 13 at two load stages, showing good agreement between analysis and experiment. The analysis verified the experimentally observed fact that the longitudinal reinforcement is in tension throughout the whole length of the beam (even in the so-called compression zones) as soon as the beam is cracked.

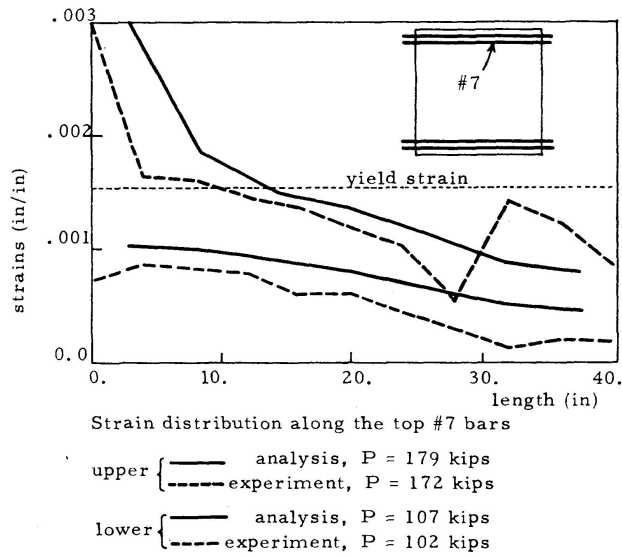


Fig. 13. Comparison of Analytical and Experimental Strains in Main Reinforcement.

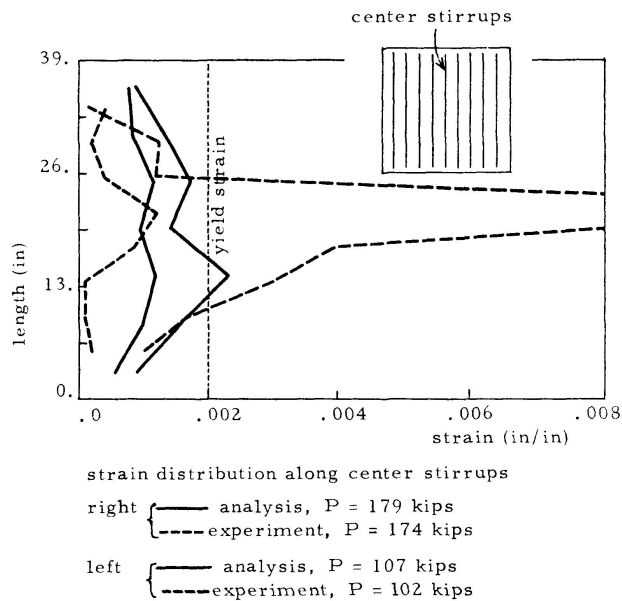


Fig. 14. Comparison of Analytical and Experimental Strains in Vertical Reinforcement.

The analytical and experimental strain distributions in the center stirrup are compared in Fig. 14 in two load stages. Here again, the discrepancy caused by different failure mechanisms is observed. The strain distribution in the analysis is much more uniform. The large strains which occur in the experimental beam at the point where the stirrup crosses the main diagonal crack do not occur in the analysis; nevertheless, the analysis indicates strains above the yield level of 0.002 in the vicinity of the diagonal crack

Conclusions

Applicability of the Finite Element Analysis

On the basis of the results presented, the following conclusions can be drawn:

1. The material stiffnesses given in an earlier paper [1] correctly represented the behavior of the reinforced concrete in a class of cases characterized by large crack regions. A comparative study confirmed that crack propagation and plasticity of materials are the most important non-linear effects in the problems with monotonically increasing load. Load-displacement relations can be accurately predicted in such cases.
2. The analysis can well predict crack locations and crack directions either by fine or by coarse mesh analyses. The crack modes used in the analysis [1] are sufficient for the monotonic loading cases and for cyclic loading cases without occurrence of plastic deformations.
3. Bending type of failure mechanism characterized by formation of plastic regions in the reinforcement and the compression concrete is well predicted by the analysis. The shear type failure mechanism characterized by opening of a large diagonal crack is not properly reproduced by the analysis.
4. For the prediction of the response to cyclic load histories, bond slip and crack surface deterioration should be included in the analysis. For cyclic loading involving yielding of the steel, an additional crack mode representing simultaneous occurrence of two cracks in different directions is necessary.

Simplification of Analysis of Planar Elements

On the basis of the limited amount of comparisons of the simplified beam analysis with the experimental and analytical results, the following conclusions can be drawn:

1. Beam analysis overestimates the stiffness of the uncracked panel. This only confirms the already well-known fact that the linear strain distribution is not applicable to deep beams.
2. Beam analysis of the cracked panel based on elastic transformed cross section excluding tension concrete well represents the average stiffness of a cracked panel.
3. Beam analysis only slightly underestimates the ultimate load of panels and can serve as a conservative estimate of panel strength for both bending and shear failures.

The conclusions imply some practical suggestions for the analysis of structures containing walls or panels. First, an elastic analysis including the cracked concrete by means of the transformed cracked section would apparently give a good estimate of the real stiffness of the cracked structure. Secondly, the

plastic hinge theory appears to be applicable to the limit analysis of wall structures (frame-shear wall systems) subject to the same limitations used in frames (shear failure must be avoided by sufficient transverse reinforcement and rotational capacity must not be exceeded).

These conclusions are made only on the basis of three panels and thus do not cover a wide range of other practical cases with various shear spans and reinforcing. Therefore, they must be considered as tentative.

The finite element analysis used in this investigation can be eventually used for a more detailed study of this problem which would lead to more conclusive suggestions for design of reinforced concrete walls.

Acknowledgement

This paper is based on part of a Ph. D. thesis by the senior author submitted to the Department of Civil Engineering, University of Colorado. Thanks are expressed to the University's Council on Research and Creative Work for financial support, to the Computing Center for computation time, and to the Department for use of the laboratory facilities. The authors also appreciate the help of Professors Paul P. Lynn and Leonard G. Tulin, University of Colorado, and of Professor Thomas Paulay, University of Canterbury.

Keywords

Cyclic load; experiment; finite element method; limit analysis; reinforced concrete; shear wall; stress analysis; structural analysis; panels; plasticity; cracking.

References

1. CERVENKA, V., and K. H. GERSTLE: Inelastic Analysis of Reinforced Concrete Panels, Part I: Theory. IABSE Publications Vol. 31-II, 1971.
2. PAULAY, T.: The Coupling of Shear Walls. Ph. D. Thesis, Department of Civil Engineering, University of Canterbury, Christchurch, New Zealand, 1969.
3. CERVENKA, V.: Inelastic Finite Element Analysis of Reinforced Concrete Panels Under In-Plane Loads. Ph. D. Thesis, Department of Civil Engineering, University of Colorado, 1970.

Summary

Inelastic finite element analysis of reinforced concrete panels is compared with experimental results. Load-displacement diagrams, crack patterns and failure mechanisms of shear wall specimens are examined under monotonic

as well as cyclic load histories. Load-displacement relations and crack patterns can be accurately predicted by the analysis for the case with monotonically increased load.

Résumé

L'analyse inélastique d'éléments finis de plaques en acier-béton est comparée aux résultats expérimentaux. Des diagrammes de déplacement de la charge, des épreuves de rupture et influences de défauts aux épreuves de cisaillement sont examinées sous charge monotonique et sous les conformités de charges cycliques. Des relations de déplacement de la charge et des épreuves de rupture se laissent prédire exactement par l'analyse pour le cas de charges uniformément élevées.

Zusammenfassung

Die unelastische Analyse endlicher Elemente von Stahlbetonscheiben wird mit den experimentellen Ergebnissen verglichen. Lastverschiebungsdiagramme, Bruchproben und Brucheffekte von Schubwandproben werden sowohl unter gleichförmiger wie unter den Gesetzmässigkeiten zyklischer Belastungen untersucht. Lastverschiebungs-Beziehungen und Bruchproben lassen sich durch die Analyse für den Fall einer gleichförmig zunehmenden Belastung genau vorhersagen.

Leere Seite
Blank page
Page vide